Available online at www.sciencedirect.com

ScienceDirect

Procedia Structural Integrity 13 (2018) 444–449

Structural Integrity Procedia

www.elsevier.com/locate/procedia

ECF22 - Loading and Environmental effects on Structural Integrity

Design of Wing Spar Cross Section for Optimum Fatigue Life

Khalid Eldwaib[a]*, Aleksandar Grbović[a], Gordana Kastratović[b], Mustafa Aldarwish[a]

[a]*Faculty of Mechanical Engineering, University of Belgrade, Kraljice Marije 16, 11120 Belgrade 35, Serbia*
[b]*Faculty of Transport and Traffic Engineering, University of Belgrade, Vojvode Stepe 305 11000 Belgrade, Serbia*

Abstract

Aircraft structure is the most obvious example where functional requirements demand light weight and strong structures. Shape and sizing optimization are being increasingly used nowadays for designing lightweight structural components. The aim of this paper is to present optimization of I-section integral wing spar made of aluminum 2024-T3. The efficient design, based on optimum fatigue life, was achieved using Extended Finite Element Method (XFEM) and its ability to simulate crack growth in complex geometry. The computations were carried out in Morfeo/Crack for Abaqus software which relies on the implementation of XFEM. Shape optimization of the aircraft wing spar beam was conducted by comparing the fatigue crack growth lives for different cross section shapes, but constant cross section area of the spar. The analysis revealed that XFEM is efficient tool for complex three-dimensional configurations optimization where extended fatigue life is one of the most important objectives.

Peer-review under responsibility of the ECF22 organizers.

Keywords: aircraft structure; optimization; Extended Finite Element Method; fatigue life.

1. Introduction

The shape optimization is being increasingly used to design lightweight structural components. It is also being used to develop localized shape strategies to restore the operational availability of ageing structural components. However, it is important to note that all new aircraft design and structural changes made to in-service aircraft require a damage tolerance analysis as outlined in the US Joint Services Structural Guidelines JSSG-2006 (1988), which states that all safety-of-flight critical structures should be designed using a damage tolerance analysis. The purpose of this requirement is to ensure that any cracks present in the structure will not cause loss of the structure for some

* Corresponding author.
E-mail address: kedwaib@yahoo.com

2452-3216
Peer-review under responsibility of the ECF22 organizers.
10.1016/j.prostr.2018.12.074

predetermined period of in-service operation. Indeed, it is essential that structures should be designed such that at no time in its operational life will the residual strength of the structure fall beneath limit load, according to Jones R. et al. (2004).

Several types of wing spar structure have been studied and optimized in the literature (Ajith V. S. et al. (2017)). The efficient design was achieved by the use of strength of material approach. Girennavar M., et al. (2017) considered a wing spar as a beam with discrete loads at different stations. The design was carried out as per the external bending moment at each station. Weight optimization of the spar was carried out by introducing lightening cut-outs in the web region. Attempt has been made by Datta, D., and Deb, K. (2006), to design the optimum cross-sections for load-carrying structures, using a multi-objective evolutionary algorithm, for simultaneously maximizing moment of inertias and minimizing the cross-sectional area. According to Jones R. et al. (2004) when designing a fatigue optimized structure, it was essential not only to reduce the peak stress but also to ensure that the critical crack lengths associated with cracks at the critical design feature were not reduced. An approach to the optimization of the thin-walled cantilever open section beams subjected to the bending and to the constrained torsion was considered by Anđelić, N., and Milošević-Mitić, V. (2007). To reduce the induced undesired stresses, a load carrying beam like wing spar should has its related area moment of inertia as large as possible. However, an increase in such moment of inertia comes with an increase in the transverse cross-sectional area and hence, the weight of the spar. Therefore, the maximization of moment of inertia should not take place at the cost of the excessive weight of the spar (Datta, D., and Deb, K. (2006)).

The aim of research presented in this work was to design an optimized shape and size of a wing spar cross section based on fatigue life obtained for fatigue crack propagation phase. The task of achieving the optimal design was carried out by maximizing moment of inertia at constant cross-section area of the wing spar. This was done through a several case studies.

2. Optimization methodology

Under service loading, characterized by many load cycles, fatigue cracks initiate from the most severe stress concentrators (i.e. riveted holes) on the differential wing spar. This has been observed in experimental work of Petrašinović, D. et al. (2012), in which fatigue life was determined for 2024-T3 spar of light aircraft. Fatigue cracks appeared in the bottom caps (flanges) and then grew in a direction perpendicular to the spar web until total caps' failure. Failure like this can lead to catastrophic consequences during the flight if the crack is not detected and cap repaired. Integral structures are more resistive to crack appearance since they don't have many stress concentrators, but their shape must be carefully chosen to provide reasonable fatigue life after the crack initiation.

Shape optimization of the integral spar was conducted by comparing the fatigue crack growth life for three different cross section shapes and same cross section area of the spar beam (idea was to keep constant mass of the spar). The first analyzed shape was I-section (used for modelling *main integral spar* – case A) with the same dimensions as the differential spar (riveted structure) used in work of Petrašinović, D. et al. (2012). The second shape was a channel-section (*U-section spar* – case B) and, finally, the third shape was I-section with intermediate cap (*I-section with a cap spar*– case C). All three shapes with dimensions are shown in Fig. 1, 2 and 3.

First two shapes are well known and are frequently used in spar design, but I-section with a cap is somehow unusual and rarely used before. This shape has additional, intermediate cap at an assumed height from the bottom cap. In the event of fatigue crack appearance at the bottom cap, this cap may fail but the top cap, web and the intermediate cap should remain intact and spar could carry designed load. In this paper, case C is represented through three subcases, all with different dimensions (size optimization was objective, too). These subcases were named C_1, C_2 and C_3. The overall dimensions of the models C_1, C_2 and C_3 are shown in Table 1.

3. Dimensions of analyzed models and applied displacements

In order to applied adequate displacements at free ends of spar beam models, moment of inertia (I) for each cross section was extracted from CATIA v5. Then, the required displacement (Δ) for each model was calculated using the well-known equation:

$$\Delta = \frac{PL^3}{3EI} \quad (1)$$

where P is the load applied on the spar (same for all models); E is the modulus of elasticity (same for all models, material 2024-T3); L is length of the spar (same for all models) and I is the moment of inertia of chosen cross section (values shown in Table 2).

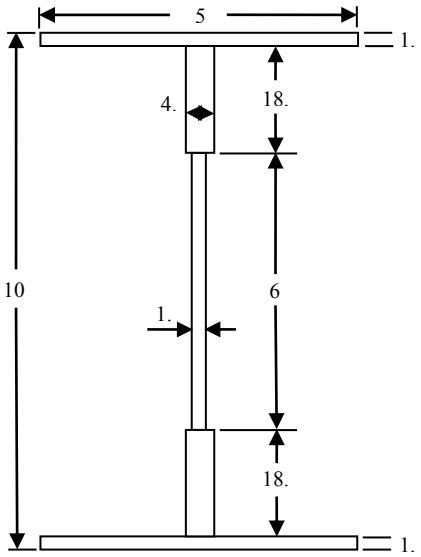

Fig. 1 Cross section of main integral spar

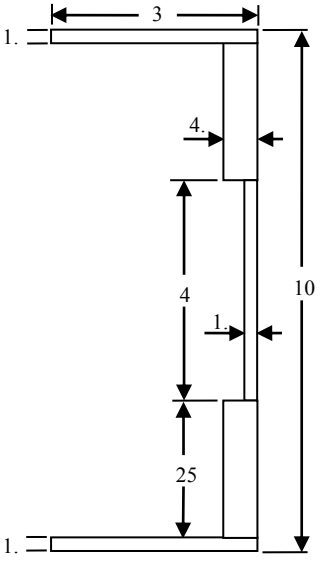

Fig. 2 Cross section of U spar

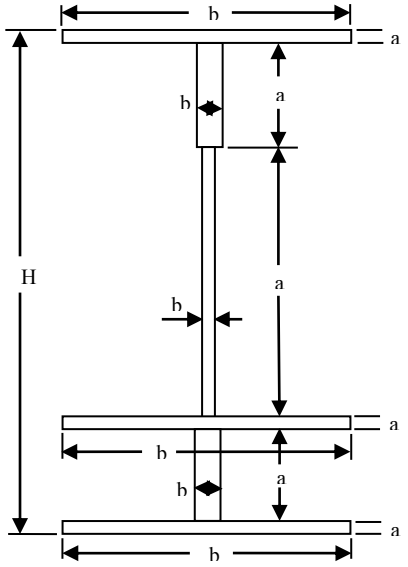

Fig. 3 Dimensions of I-section with intermediate cap

Table 1 The overall dimensions for I-section with a cap spar (shown in Figure 3).

Case	a_1	b_1	a_2	b_2	a_3	b_3	a_4	b_4	a_5	b_5	H
C_1	1.6	41.0	1.6	21.0	13.4	4.2	23.4	4.2	58.4	1.0	100.0
C_2	1.6	54.7	1.6	54.7	5.0	3.0	5.0	3.0	85.2	1.0	100.0
C_3	1.6	53.6	1.6	53.6	5.0	3.0	5.0	3.0	90.2	1.0	105.0

All dimensions in mm

Table 2 Moments of inertia and appropriate displacements for different spars

Spar category (type)	No.	Case No.	I (mm^4)	Displacement (mm)
Main integral spar	1	Case A	654,900	3.000
U-section spar	2	Case B	558,300	3.519
I-section with a cap spar	3	Case C_1	583,500	3.367
	4	Case C_2	662,000	2.968
	5	Case C_3	726,300	2.705

Value of displacement 3mm for main integral spar was chosen because exactly the same displacement was observed in experimental work of Petrašinović, D. et al. (2012).

4. Results of fatigue crack growth simulations

All simulations of cracks' growths were performed using *Morfeo/Crack for Abaqus* software. This software was verified by many authors including Eldwaib, K. A. et al. (2017), and it proved to be useful tool in fatigue crack propagation analyses. In the analyses of defined spar models, the fatigue crack initiation stage was ignored since the emphasis was on the crack growth phase only. Two initial penny shaped cracks were inserted in all cases: one in the right lower cap (flange) and another in the left lower cap next to fixed end of the spar beam, where the most severe

stress concentration occurs. Two cracks were propagated simultaneously in cases A and C because in work of Petrašinović, D. et al. (2012) two cracks appeared on lower caps during the experiment with aluminium spar. In the case B one initial crack was used because U-section spar had only one lower cap. In this paper comparisons are made for cracks initiated at the same spots (left lower cap). To determine the number of cycles of displacement that will grow cracks to certain lengths, Paris law was integrated (Schijve, J. (2008)) using material coefficients $m = 3.2$ and $C = 2.382 \times 10^{-12}$ and stress ratio $R = 0.15$. Values of fatigue life obtained in simulations were later used to attain the optimized shape and size of the spar cross sections.

4.1 Comparison of fatigue lives (no. of cycles) for different cases

The variation of crack length "*a*" vs. number of cycles "*N*" of applied displacement is shown in Figure 4 for all analysed cases. It can be seen that the shortest fatigue life was obtained in case B where moment of inertia of spar beam cross section was lowest (558,300mm^4) and the applied displacement was highest (3.519mm). There is almost constant difference (approximately 100,000) between number of cycles in case A and case B, from cracks' lengths 2 mm up to 21mm. Although the moment of inertia in case C_1 is little bit higher than in case B and displacement is approximately 12% higher than in case A (see Table 2), number of cycles in C_1 is a bit less than number in A, with the difference 5,000 – 20,000 cycles during the cracks' growth. This is result of C_1 geometry consistency and is a direct consequence of reinforcement achieved by adding additional flange above the lower flange.

In case C_2 number of cycles was little bit less than that in case A until cracks reached 6mm; after that, number of cycles in case C_2 started to be bigger and bigger and for length 20mm difference was about 94,000 cycles. This was result of modifications in the size and position of intermediate flange (see Table 1) that led to stronger spar and more fatigue resistant lower area of cross section. It is worth mentioning that there was no significant difference in moments of inertia in cases C_2 and A and, consequently, applied displacement were almost the same.

Finally, Figure 4 shows that the longest fatigue life occurred in case C_3 for which number of cycles at a=21mm is more than 1,000,000 cycles bigger than that in Case A. This fatigue life was obtained after height H of cross section C_2 was increased from 100mm to 105mm (see Table 1) along with the increase of dimension a_5 from 85.2mm to 90.2mm. Newly obtained cross section C_3 had significantly larger moment of inertia and consequently lower displacement (Δ=2.705mm) which – at the end of the day – led to the longest fatigue life.

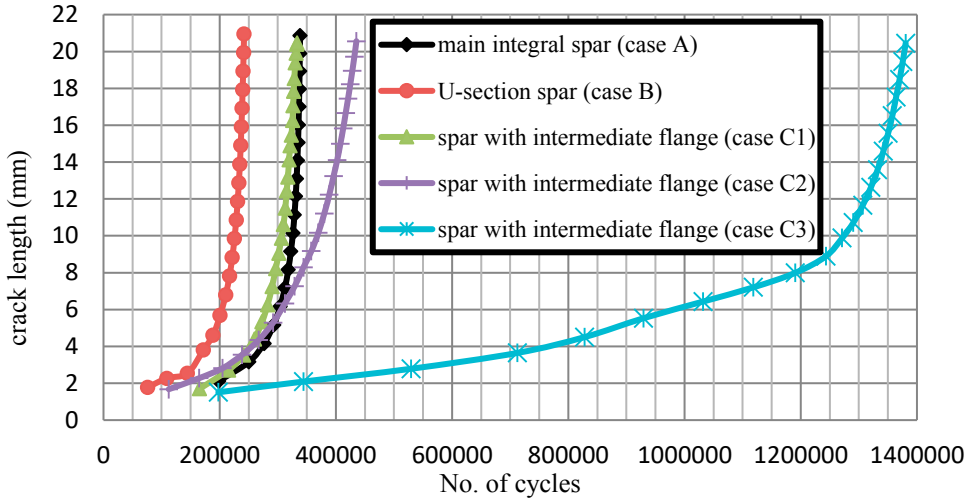

Fig. 4 Comparison of the fatigue lives (number of load cycles) for different cases

4.2 Comparison of fatigue crack growth rates (da/dN) for different cases

The slope of the crack growth curve da/dN (better known as *crack growth rate* - CGR) is good indicator of how damaged structure is going to behave under given loading conditions. Using the data obtained from *Abaqus*, i.e. the coordinates of the nodes on the crack front and number of cycles evaluated for each (incremental) step of crack propagation, da/dN for each case was estimated. For that purpose, equation (2) was used:

$$\left(\frac{da}{dN}\right)_i = \frac{(a_{i+1}-a_i)}{N_{cycles}} \quad (2)$$

where $\left(\frac{da}{dN}\right)_i$ is crack growth rate per each propagation step; i is step number, and N_{cycles} is number of estimated load cycles per each step. Obtained results are presented in Figure 5 and Figure 6

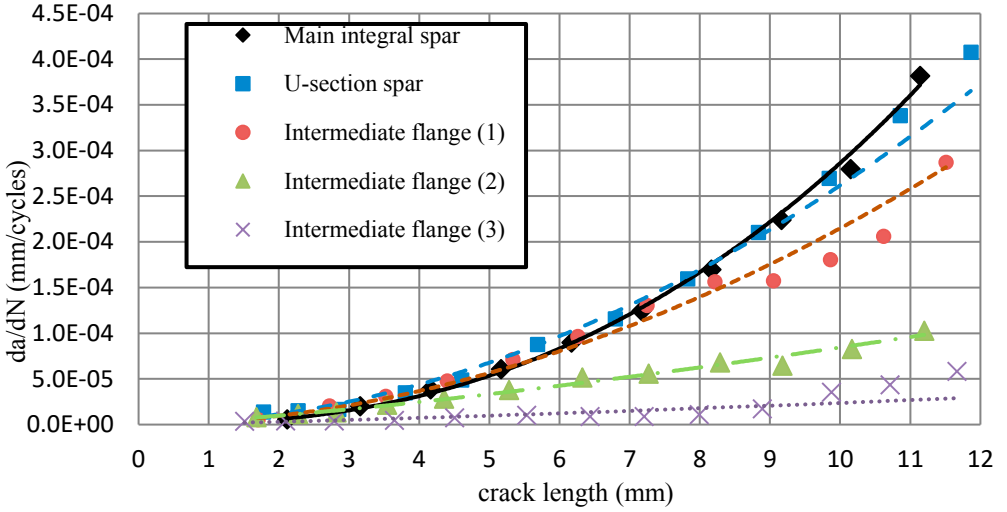

Fig. 5 Comparison of da/dN calculated per each step of crack propagation (crack length 0 – 12mm)

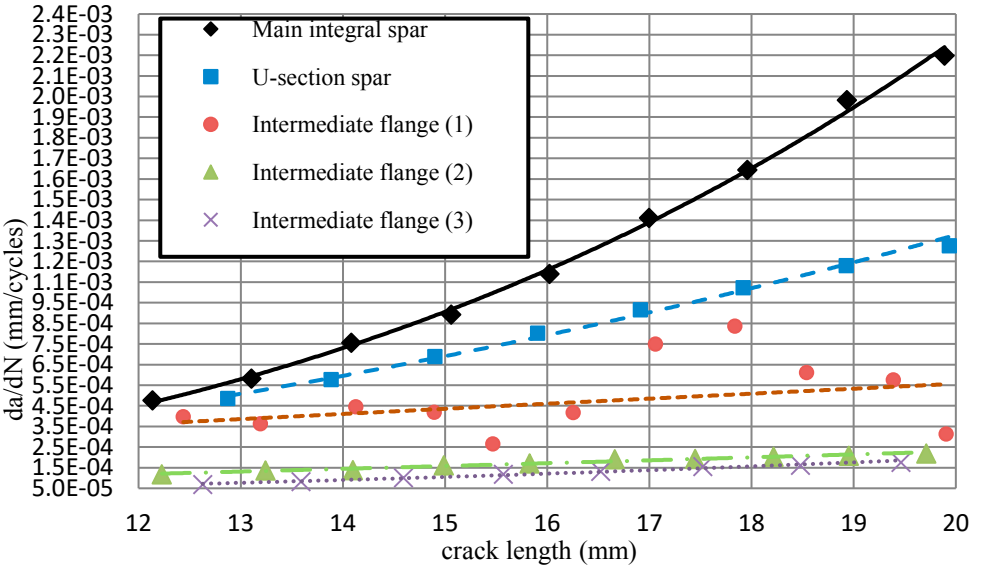

Fig. 6 Comparison of da/dN calculated per each step of crack propagation (crack length 12 – 20mm)

In Figures 5 and 6 significantly higher CGR values can be observed for cases A, B, and C_1, compared to small CGRs in cases C_2 and C_3. For small cracks' lengths (Fig. 5), differences in CGR values are not significant, but after 3mm cases C_2 and C_3 become very different from the other three. Cases A, B and C_1 have similar CGR values until 8 mm and then main integral spar values (case A) start to grow faster than the others. Differences become even greater when cracks reach lengths higher than 12mm (Fig. 6), while the greatest difference can be seen at a=20mm: CGR in case C_3 is about $2 \times 10^{-4}\, mm/cycle$, though CGR in case A is almost ten times bigger ($2.2 \times 10^{-3}\, mm/cycle$).

It should be noted that in the cases where two cracks were propagated simultaneously (A, C_1, C_2, C_3) behaviour of the second crack (on the lower right cap) varied from case to case. For example, in case C_2 second crack met first (Figure 7) after 27 steps of propagation (cracks were propagated in steps of approximately 1mm in all five cases) and newly formed crack continued to grow in vertical spar wall, while in case A deformation of the spar prevented the growth of the second crack after 8 steps. All these findings prove that geometry of cross section significantly influences fatigue life of damaged structure; therefore, this matter clearly needs to be given more attention in the future.

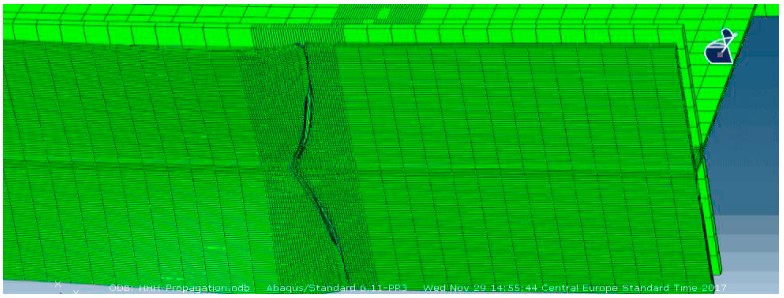

Fig. 7 Two cracks met on the bottom cap (case C_2)

5. Conclusions

In aircraft design, cracks' appearance on the wing parts is allowed (as defined in so-called *fail-safe design philosophy*), but life until critical crack length must be evaluated with high confidence in order to prevent undesirable consequences. That's not an easy job because in most cases cracks appear on parts with complex geometry subjected to variable loads during service and data on critical lengths are generally available only for simpler load/geometry configurations. This is reason why emphasis – in a research presented here – was on developing XFEM based computational method for successful crack growth life estimation. On the other hand, main goal was to obtain optimized size and shape (for given mass of the spar) that will significantly extend fatigue life.

Five different shapes had been analysed (I-section, U-section and three variants of I-section with intermediate cap (flange)) and it was found that the optimum spar with the longest crack growth life and the lowest crack growth rate had I-section with intermediate cap shape (case C_3). Fatigue life of this spar was nearly 1,400,000 cycles, while in the next best case (C_2) life was significantly shorter (450,000 cycles). Typical I-section had the lowest fatigue life (250,000 cycles) and let's not forget that this is spar shape used in more than 90% of the light airplanes nowadays.

As the results of this research suggest, to increase fatigue life of light aircraft spar with intermediate cap should be used. It was proven that in the event of crack initiation at the bottom cap, where cracks usually appear, this cap will fail sooner or later, but the top cap, web and the intermediate cap will remain intact and spar could carry designed load much longer than any other configuration.

References

JSSG-2006, Joint Service Specification Guide, Aircraft Structures, Dept. of Defense, October 1988.

Ajith, V. S., Paramasivam R., Vidhya, K. (2017). Study of optimal design of spar beam for the wing of an aircraft. International Journal of Engineering Development and Research, 5(3), 179-193.

Jones, R., Pitt, S., & Peng, D. (2004). Structural optimisation for light weight durable structures. In Structural Integrity and Fracture International Conference (SIF'04) (pp. 171-178).

Datta, D., and Deb, K. (2006). Design of optimum cross-sections for load-carrying members using multi-objective evolutionary algorithms. Int. J. of Systemics, Cybernetics and Informatics (IJSCI), 57-63.

Girennavar M., et al. (2017). Design, Analysis and Testing of Wing Spar for Optimum Weight. International Journal of Research and Scientific Innovation (IJRSI), Volume IV, Issue VII, 104-112.

Anđelić, N., and Milošević-Mitić, V. (2007). An approach to the optimization of thin-walled cantilever open section beams. Theoretical and applied mechanics, 34(4), 323-340.

Eldwaib, K. A., Grbovic, A., Kastratovic, G., Radu, D., Sedmak, S. (2017). Fatigue life estimation of CCT specimen using XFEM. Structural Integrity and Life, 17(2), 151-156.

Petrašinović, D., Rašuo, B., Petrašinović, N. (2012). Extended finite element method (XFEM) applied to aircraft duralumin spar fatigue life estimation. Technical Gazette, 19(3), 557-562.

Schijve, J., Fatigue of Structures and Materials, 2nd edition, Springer (2008).